Radiology: Imaging Cancer

ORIGINAL RESEARCH

Radiologic-Pathologic Correlation of Nonmass Enhancement Contiguous with Malignant Index Breast Cancer Masses at Preoperative Breast MRI

*Derek L. Nguyen, MD** • *Mira Lotfalla, MBBCh** • *Ashley Cimino-Mathews, MD* • *Mehran Habibi, MD* • *Emily B. Ambinder, MD*

From the Department of Radiology, Duke University Medical Center, Durham, NC (D.L.N.); Department of Pathology, University of South Florida Health Morsani College of Medicine, Tampa, Fla (M.L.); and Department of Pathology (A.C.M.), Department of Surgery (M.H.), and Russell H. Morgan Department of Radiology and Radiological Science (E.B.A.), Johns Hopkins Medicine, 601 N Caroline St, Baltimore, MD 21287. Received May 2, 2023; revision requested June 4; revision received October 4; accepted December 15. **Address correspondence to** E.B.A. (email: *emcinto8@jhmi.edu*).

* D.L.N. and M.L. contributed equally to this work.

E.B.A. receives grant funding from The Nexus Fund and a Radiological Society of North America Research Scholar Grant for activities not related to the topic of this article.

Conflicts of interest are listed at the end of this article.

See also the commentary by Newell in this issue.

Radiology: Imaging Cancer 2024; 6(2):e230060 • https://doi.org/10.1148/rycan.230060 • Content codes: BR MR OI

Purpose: To determine the pathologic features of nonmass enhancement (NME) directly adjacent to biopsy-proven malignant masses (index masses) at preoperative MRI and determine imaging characteristics that are associated with a malignant pathologic condition.

Materials and Methods: This retrospective study involved the review of breast MRI and mammography examinations performed for evaluating disease extent in patients newly diagnosed with breast cancer from July 1, 2016, to September 30, 2019. Inclusion criteria were limited to patients with an index mass and the presence of NME extending directly from the mass margins. Wilcoxon rank sum test, Fisher exact test, and χ^2 test were used to analyze cancer, patient, and imaging characteristics associated with the NME diagnosis.

Results: Fifty-eight patients (mean age, 58 years ± 12 [SD]; all women) were included. Malignant pathologic findings for mass-associated NME occurred in 64% (37 of 58) of patients, 43% (16 of 37) with ductal carcinoma in situ and 57% (21 of 37) with invasive carcinoma. NME was more likely to be malignant when associated with an index cancer that had a low Ki-67 index (<20%) ($P = .04$). The presence of calcifications at mammography correlating with mass-associated NME was not significantly associated with malignant pathologic conditions ($P = .19$). The span of suspicious enhancement measured at MRI overestimated the true span of disease at histologic evaluation ($P < .001$), while there was no evidence of a difference between span of calcifications at mammography and true span of disease at histologic evaluation ($P = .27$).

Conclusion: Mass-associated NME at preoperative MRI was malignant in most patients with newly diagnosed breast cancer. The span of suspicious enhancement measured at MRI overestimated the true span of disease found at histologic evaluation.

More than 280 000 women in the United States will be newly diagnosed with invasive breast cancer this year, the majority of whom are candidates for breast-conserving surgery (1). There is increasing use of breast MRI for preoperative evaluation of disease extent. Breast MRI and mammography have similar positive predictive values for the detection of breast cancer (2). However, breast MRI has better sensitivity and negative predictive values than mammography for detecting the local extent of the known primary malignancy and synchronous ipsilateral or contralateral lesions following initial diagnosis, thus influencing surgical planning (2,3). While the use of preoperative breast MRI has led to the reduction of local recurrence rates by at least 5% in patients undergoing breast conservation surgery (4), it has also led to an increase in the rate of wider surgical margins or conversion to mastectomies in up to 12.5% of cases because of additional MRI findings suspicious for malignancy, resulting in an unnecessary upgrade in surgical excisions in about 5%–6% of cases (5–7).

Additional enhancing findings at preoperative MRI examinations raise concerns for breast radiologists and surgeons, as patients newly diagnosed with breast cancer have a higher incidence of additional areas of cancer (8,9). Nonmass enhancement (NME) is the most common of these additional findings. NME is associated with malignant calcifications and is the MRI finding most suggestive of ductal carcinoma in situ (DCIS) (9–12). Furthermore, NME adjacent to a biopsy-proven malignancy (index cancer) at preoperative breast MRI has been associated with higher rates of positive resection margins (13,14). However, given the low specificity of breast MRI in the diagnosis of breast cancer, management of these findings is controversial because NME is the most common cause of false-positive findings at breast MRI (5,15). There is minimal evidence-based literature on the management of NME directly adjacent to malignant index masses at preoperative MRI in candidates for breast conservation surgery, leading to additional, potentially unnecessary, imaging, biopsies, conversion to mastectomies, or wider excisions in these patients (5).

Abbreviations

DCIS = ductal carcinoma in situ, NME = nonmass enhancement

Summary

Nonmass enhancement directly adjacent to malignant index breast cancer masses yielded malignant pathologic findings in more than half of cases.

Key Points

- The total span of mass-associated nonmass enhancement (NME) contiguous with the primary index malignancy at preoperative MRI overestimated the true histologic span of disease in patients newly diagnosed with breast cancer (span at MRI: 4.9 cm ± 2.1 [SD], span at pathologic analysis: 3.0 cm ± 2.4; $P < .001$).
- NME was more likely to be malignant when associated with an index cancer that had a low Ki-67 index (<20%) ($P = .04$).

Keywords

Breast, Mammography

Determining the clinical significance of mass-associated NME at preoperative breast MRI examinations can help guide surgical planning in patients who are potential candidates for breast conservation surgery. Therefore, establishing more evidence-based preoperative recommendations for these patients is relevant and will improve the quality of patient care. The objective of this study is to provide evidence to inform surgical decision-making in patients with newly diagnosed breast cancer masses. This study aims to determine the pathologic findings of NME contiguous with malignant index masses at preoperative MRI and the imaging characteristics that are associated with malignant NME.

Materials and Methods

Patients and Study Design

The institutional review board reviewed this study and designated it as falling under exempt status under the Department of Health and Human Services regulations. Protected health information was stored on a virtual desktop (Secure Analytic Framework Environment, or SAFE, desktop) that is a part of our institution's (Johns Hopkins Medicine) secure environment, where chart review and statistical analysis were performed. This study complied with the Health Insurance Portability and Accountability Act.

A retrospective cohort study was performed to review the data from all breast MRI and mammography examinations performed at our institution between July 1, 2016, and September 30, 2019, in patients with newly diagnosed breast cancer for the evaluation of disease extent. Inclusion criteria were limited to patients with a malignant index mass and mass-associated NME, which was defined as the presence of NME extending directly from the mass margins and no other ipsilateral or contralateral NME findings. Patients treated with neoadjuvant chemotherapy were included if they had undergone an MRI-guided biopsy of the mass-associated NME prior to starting treatment. Exclusion criteria were patients with breast cancer without a dominant mass, no mass-associated NME, malignant index mass not visualized at preoperative MRI, and patients treated with neoadjuvant chemotherapy who did not undergo MRI-guided biopsy of the mass-associated NME prior to initiating treatment.

Data Extraction and Evaluation

Current Procedural Terminology codes were used to identify breast MRI examinations performed during our study period. Our institution's value analytics team then extracted the corresponding patient medical record numbers and age at the time of examination from our institution's electronic medical record (Epic EMR system; Epic Systems).

Manual chart review was performed for each patient to record breast cancer characteristics, including histologic type, molecular subtype, and initial treatment performed (lumpectomy, mastectomy, or neoadjuvant chemotherapy). Histologic types were recorded using standard classifications (16). Benign lesions were defined as benign breast tissue and pseudoangiomatous stromal hyperplasia. High-risk lesions were defined as atypical ductal hyperplasia, atypical lobular hyperplasia, lobular carcinoma in situ, radial scar, complex sclerosing lesion, or papillary lesion. Malignant lesions included DCIS and invasive carcinoma. All malignant lesions in our cohort were managed by surgical excision, and no patient underwent active surveillance for their malignant diagnosis. Additional grouping classifications are detailed as follows: Microinvasive DCIS and all subtypes of invasive ductal carcinoma, such as mucinous or papillary, were classified as invasive ductal carcinoma in our study. Additional cancer features, including hormone receptor status, human epidermal growth factor 2 status, and Ki-67 level, were also extracted from the medical record and measured specifically from the overall malignant mass. Ki-67 level was quantified using standard immunohistochemistry techniques: fixation with 10% buffered formalin, routine tissue processing with paraffin embedding, and Ki-67 detection using Ventana iVIEW (Roche Diagnostics). Ki-67 levels were categorized as high (≥20%) or low (<20%) (17).

The original breast MRI reports were dictated by 11 breast imaging radiologists with experience ranging from 2 to 35 years. Manual chart and imaging review was performed by one of the authors (D.L.N., postgraduate year 5 diagnostic radiology resident) for each included patient. The reader reviewed the characteristics of the malignant index mass (size, shape, margins, internal enhancement, and kinetics) and mass-associated NME (size, distribution, internal enhancement pattern, and kinetics), as well as the final histologic diagnosis of MRI-guided biopsy of the mass-associated NME. The same author recorded the largest size dimension of the malignant index mass, mass-associated NME, and total imaging span (malignant index mass and mass-associated NME) on the first axial postcontrast T1-weighted fat-saturation subtraction sequence. The recorded terminology of the mass and NME descriptors were those used in the Breast Imaging Reporting and Data System (ie, BI-RADS) atlas, 5th edition (18). Whether the presence of mass-associated NME at breast MRI changed the initial surgical treatment plan from lumpectomy to total mastectomy for the patient was also recorded. All patients in our cohort underwent either lumpectomy or mastectomy.

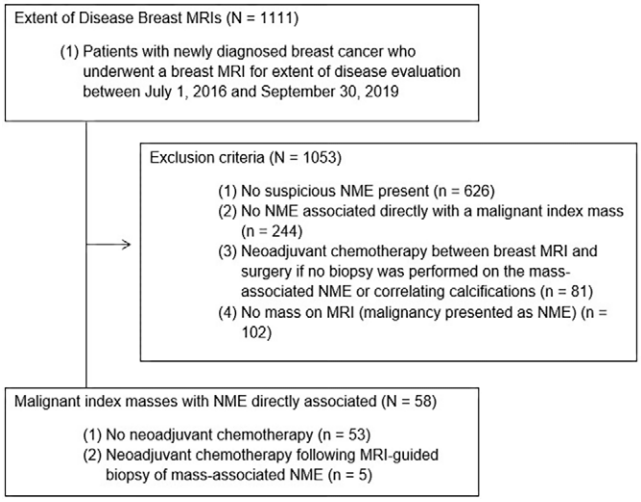

Figure 1: Flowchart of patients included in this retrospective cohort study. NME = nonmass enhancement.

Manual chart review was performed by the same author (D.L.N.) to determine if a diagnostic mammogram was acquired within 2 months prior to the preoperative breast MRI examination for each included patient. All mammography examinations were performed with a digital breast tomosynthesis mammography unit (Selenia Dimension; Hologic). The following characteristics were also recorded: *(a)* presence of calcifications on the diagnostic mammogram that were directly associated with the malignant index mass and if this distribution correlated with the mass-associated NME observed on the preoperative breast MR image, *(b)* total imaging span of both the malignant index mass and the calcifications, and *(c)* final histologic diagnosis of stereotactic-guided biopsy of the calcifications that correlated with the mass-associated NME. The same author recorded the largest size dimension of the calcifications that correlated with the mass-associated NME on either the craniocaudal or mediolateral oblique view, whichever was the longest.

Pathology slides of all cases were retrospectively re-evaluated by a breast pathologist (one of the authors: M.L.) for histologic correlation of the NME that was directly contiguous with the malignant index mass. For each case, the pathologist was provided the size, distribution, and location of the mass-associated NME, from the preoperative breast MRI examination, relative to the index malignant mass to determine if a pathologic correlate existed in the surgical specimen (from lumpectomy or mastectomy). Total span of disease was defined as the total size of both the malignant index mass and the surrounding malignancy measured in the specimen by the breast pathologist (one of the authors). For cases without available pathology slides, histologic correlation was determined by the breast pathologist (M.L.) from the pathology report instead (n = 12). These cases, as well as the cases with neoadjuvant chemotherapy following MRI-guided biopsy of the mass-associated NME (n = 5), were excluded from the analysis of the span of disease, given that there was no direct pathologist evaluation.

Breast MRI Technique

Breast MRI examinations were performed with either a 1.5-T Discovery (GE HealthCare), a 3-T Skyra (Siemens Healthineers), or a 3-T Trio (Siemens Healthineers) scanner using a 16-channel breast coil (Sentinelle; InVivo) with patients in the prone position. Diagnostic examinations included three postcontrast sequences acquired for 120 seconds each 30 seconds after the administration of 0.1 mmol of gadolinium-based contrast agent per kilogram of body weight at a rate of 2 mL/sec followed by a 20-mL saline flush. Specific subtraction sequences were performed by subtracting the precontrast T1-weighted fat-saturated sequence from the postcontrast T1-weighted fat-saturated sequence for all three postcontrast sequences. Maximum intensity projection in 360° rotation was created based on the first postcontrast T1-weighted fat-saturated subtraction sequence. Dynamic contrast-enhancement kinetics was evaluated using an external software program (DynaCAD; Philips Healthcare) that characterized dynamic enhancement patterns of each pixel above threshold as persistent, plateau, or washout.

Statistical Analysis

All statistical analyses were performed using computing software program R 2017 (R Foundation for Statistical Computing). Mass-associated NME positive for malignancy was defined as a pathologic result of DCIS or invasive carcinoma. Associations between patient and imaging characteristics with the mass-associated NME diagnosis (benign and high-risk or malignant) were assessed using Wilcoxon rank sum test for continuous variables and χ^2 test or Fisher exact test for categorical variables. Wilcoxon signed rank test was used to compare the span of suspicious enhancement at MRI and the span of correlating calcifications with the true pathologic span of disease. The mean and difference were calculated for each pair of measurements, and these were used to form Bland-Altman plots with 95% CIs. We also present the frequency, with percentage in parentheses, of patients with an MRI enhancement span or calcification span within 1 cm and 2 cm of the true pathologic span of disease. P value less than .05 indicated a statistically significant difference.

Results

Patient Characteristics

A total of 1111 MRI examinations with an indication for extent of disease were performed during the study period. There were 58 unique patients (all female) with a mean age of 58.0 years ± 12.0 [SD] who met the criteria for this study (Fig 1). All included patients had an index breast cancer with contiguous NME at preoperative MRI. Patients were categorized into two distinct groups on the basis of whether the final pathologic analysis outcome for the NME was benign and high risk (n = 21) or malignant (n = 37). There was no evidence of a difference in patient age (58 years ± 14 vs 58 years ± 11, respectively; P = .59) between the two groups. Radiologic-pathologic examples are shown in Figure 2.

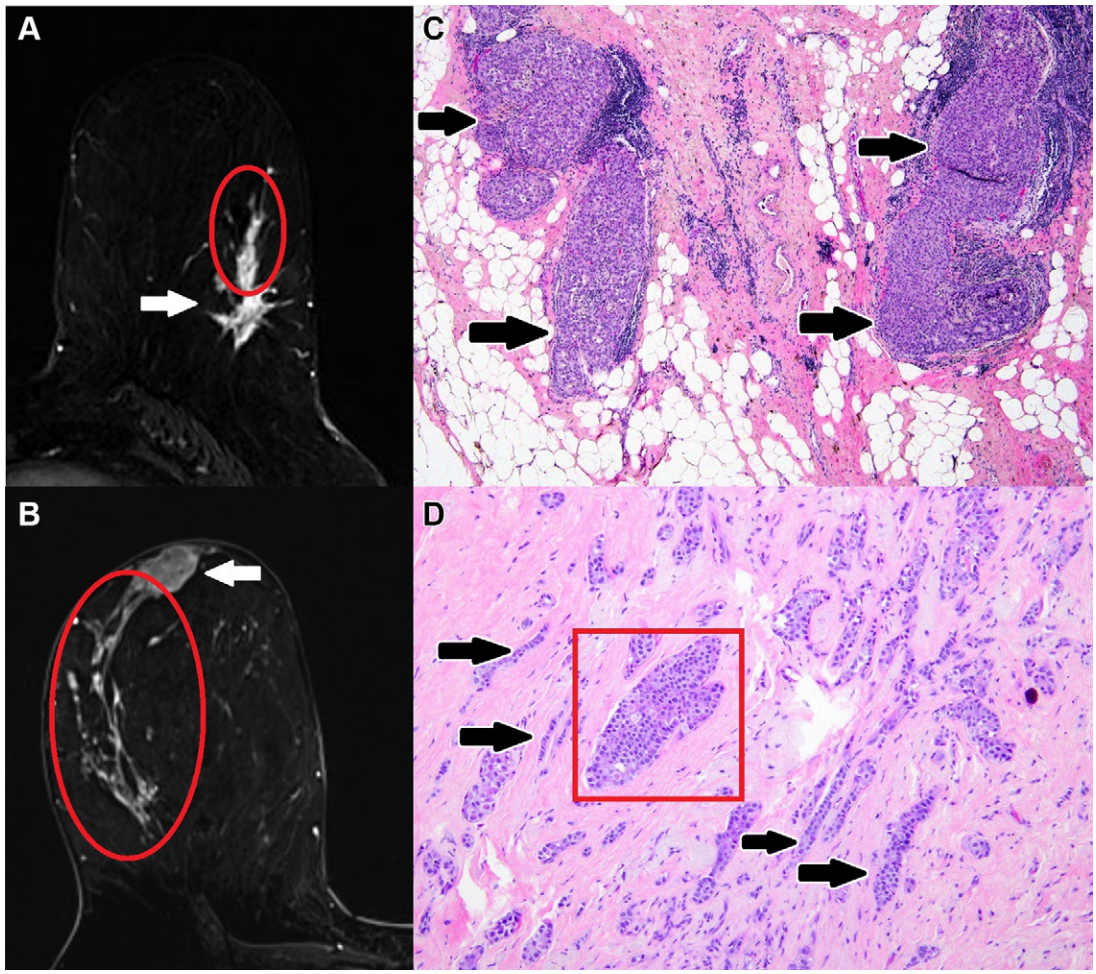

Figure 2: Examples of malignant mass-associated nonmass enhancement (NME): Axial breast MR images (left) of malignant mass-associated NME (red oval) and corresponding pathology slides (right). **(A, C)** Mass-associated NME that was MRI-guided biopsy–proven ductal carcinoma in situ (DCIS) in a 62-year-old woman with newly diagnosed invasive ductal carcinoma. Axial postcontrast T1-weighted subtraction image **(A)** demonstrates a 2.2-cm heterogeneous NME in a linear distribution extending from a 2.0-cm irregular heterogeneous mass with spiculated margins in the lower outer left breast. Histologic view of the mass-associated NME shows dilated ducts that are distended and filled by a solid proliferation of tumor cells (black arrows in **C**), compatible with DCIS. (Hematoxylin-eosin stain; original magnification, ×40.) **(B, D)** Mass-associated NME that was lumpectomy-proven invasive lobular carcinoma and lobular carcinoma in situ in a 43-year-old woman with newly diagnosed invasive lobular carcinoma. Axial postcontrast T1-weighted subtraction image **(B)** demonstrates a 10.0-cm clumped NME in a segmental distribution extending from a 2.3-cm oval heterogeneous mass with irregular margins in the upper outer right breast. Histologic view of mass-associated NME shows a dilated duct filled by an intraductal proliferation of monotonous loosely cohesive cells (red box in **D**), compatible with lobular carcinoma in situ, and infiltrative proliferation of mildly atypical cells arranged in single files, cords, and single cells in a desmoplastic stroma (black arrows in **D**), compatible with invasive lobular carcinoma. (Hematoxylin-eosin stain; original magnification, ×100.)

Mass-associated NME Characteristics

Pathologic findings for NME contiguous with malignant index masses was confirmed with MRI-guided core biopsy (n = 15), stereotactic-guided core biopsy of correlating calcifications (n = 6), or with surgical intervention (lumpectomy [n = 11] and mastectomy [n = 26]).

Pathologic findings were malignant for mass-associated NME in 64% (37 of 58) of studies: 43% (16 of 37) with DCIS and 57% (21 of 37) with invasive carcinoma. Of the 21 cases with nonmalignant mass-associated NME, 18 were benign breast tissue, two were lobular carcinoma in situ and one was pseudoangiomatous stromal hyperplasia.

Of the 53 patients who underwent upfront surgical management, 37 underwent mastectomy and 16 underwent lumpectomy. Mass-associated NME at breast MRI changed the initial planned treatment of lumpectomy to mastectomy for 59% (31 of 53) of patients. Of these patients, 74% (23 of 31) had malignant mass-associated NME outcomes, 52% (12 of 23) with DCIS and 48% (11 of 23) with invasive carcinoma. Of the 16 patients who underwent lumpectomy, 25% (four of 16) had positive margins and required repeat excision.

Tables 1 and 2 present factors associated with the final pathologic condition outcome of NME contiguous with the index breast mass (benign and high risk or malignant). Table 1 includes features of the index breast mass, and Table 2 includes features of the NME. No imaging feature was associated with malignant pathologic findings (Table 2). Low

Table 1: Features of Malignant Index Breast Masses and Association with Pathologic Outcome of Contiguous Nonmass Enhancement at Preoperative Breast MRI

Characteristic of Index Breast Cancer	Final Pathologic Outcome		*P* Value
	Benign and High-Risk NME (*n* = 21)	Malignant NME (*n* = 37)	
Histologic subtype			>.99
Invasive ductal carcinoma	16 (76)	29 (78)	
Invasive lobular carcinoma	5 (24)	8 (22)	
Estrogen receptor			>.99
Negative	2 (9.5)	3 (8.1)	
Positive	19 (90)	34 (92)	
Progesterone receptor			.37
Negative	4 (19)	11 (30)	
Positive	17 (81)	26 (70)	
Human epidermal growth factor receptor 2			>.99
Negative	16 (76)	29 (78)	
Positive	5 (24)	8 (22)	
Ki-67 index			.04
<20%	5 (28)	15 (60)	
≥20%	13 (72)	10 (40)	
Unknown†	3	12	
Mass diameter measured at MRI (cm)*	2.1 (1.1)	1.8 (1.2)	.70
Mass shape at MRI			.12
Irregular	16 (76)	34 (92)	
Oval	3 (14)	3 (8.1)	
Round	2 (9.5)	0 (0)	
Mass margin at MRI			.49
Irregular	17 (81)	27 (73)	
Spiculated	4 (19)	10 (27)	
Mass enhancement pattern at MRI			.61
Heterogeneous	15 (71)	24 (65)	
Homogeneous	6 (29)	13 (35)	
Mass kinetics			.24
Type 1	16 (89)	24 (71)	
Type 2 or 3	2 (11)	10 (29)	
Unknown‡	3	3	

Note.—Unless otherwise noted, values are numbers, with percentages in parentheses. *P* values were determined by using Wilcoxon rank sum test, Fisher exact test, and Pearson χ^2 test. NME = nonmass enhancement.

*Values are medians, with IQRs in parentheses.

† These patients were not included when calculating percentages for Ki-67 indexes <20% and ≥20%.

‡ These patients were not included when calculating percentages for type 1–3 kinetics.

Ki-67 proliferation index was associated with malignant NME (*P* = .04).

Calcifications Correlation with Mass-associated NME

Mass-associated NME correlated with mammographic calcification in 40% (23 of 58) of patients, with the median calcifications span being a shorter length than the corresponding median NME span (calcification span: 2.6 cm, IQR 1.6; NME span: 4.0 cm, IQR 2.9; *P* = .001). Radiologic-pathologic examples are shown in Figure 3. Most of the cases with corresponding calcifications were malignant (74% [17 of 23]: DCIS, 41% [seven of 17] and invasive carcinoma, 59% [10 of 17]). The presence of calcifications was not associated with malignant pathologic findings (*P* = .19).

Table 2: Features of Nonmass Enhancement Contiguous with Index Breast Cancer at MRI and Association with Final Pathologic Outcome

Characteristic of NME	Final Pathologic Outcome: Benign and High-Risk NME (n = 21)	Final Pathologic Outcome: Malignant NME (n = 37)	P Value
NME distribution			.07
Focal	1 (4.8)	0 (0)	
Linear	11 (52)	10 (27)	
Regional	0 (0)	1 (2.7)	
Segmental	9 (43)	26 (70)	
NME enhancement pattern			.58
Clumped	13 (62)	28 (76)	
Heterogeneous	3 (14)	4 (11)	
Homogeneous	5 (24)	5 (14)	
NME kinetics			.18
Type 1	16 (89)	24 (71)	
Type 2 or 3	2 (11)	10 (29)	
Unknown†	3	3	
Span of suspicious enhancement at MRI (cm)*	3.9 (1.7)	5.1 (2.7)	.06
Mammographic calcification correlate for NME			.19
None	15 (71)	20 (54)	
Present	6 (29)	17 (46)	
Span of correlating calcifications at mammography (cm)*	2.1 (1.2)	3.0 (2.7)	.06
Span of true disease at pathologic analysis (cm)*	2.1 (1.0)	2.7 (2.7)	.17

Note.—Unless otherwise noted, values are numbers, with percentages in parentheses. P values were determined by using Wilcoxon rank sum test, Fisher exact test, and Pearson χ^2 test. NME = nonmass enhancement.
* Values are medians, with IQRs in parentheses.
† These patients were not included when calculating percentages for type 1–3 kinetics.

Pathologic Analysis Specimen Correlation with Mass-associated NME and Associated Calcifications

Total span of disease at pathologic analysis was available for 79% (46 of 58) of patients. The median span of suspicious enhancement measured at breast MRI overestimated the true span of disease at histologic evaluation (MRI span: 4.0 cm, IQR 2.9; pathologic span: 2.7 cm, IQR 2.6; P = .01). Fifteen (33%) of these 46 patients had an MRI span within 1 cm of the true pathologic span, and 24 (52%) had an MRI span within 2 cm of the true pathologic span. Calcification correlation was present in 41% of these patients (19 of 46). There was no evidence of a difference between median calcification span and the true span of disease at histologic evaluation (P = .41). Fifteen (79%) of the 19 patients had a calcification span within 1 cm of the true pathologic span, and 18 of 19 (95%) had a calcification span within 2 cm of the true pathologic span. Figure 4 shows a scatterplot of the imaging span of suspicious findings (NME at MRI and calcifications at mammography) versus the true span of disease at histologic analysis. Figures 5 and 6 show the corresponding Bland-Altman plots.

Discussion

This study evaluated the pathologic findings of NME directly adjacent to malignant index masses at preoperative MRI and determined imaging characteristics associated with malignancy. NME contiguous with a malignant index mass was malignant in about two-thirds of cases (64%). The span of suspicious enhancement measured at breast MRI overestimated the true span of disease found at histologic evaluation, while we found no evidence of a difference between the span of correlating calcifications and the true span of disease at histologic evaluation.

Gweon et al (19) determined that human epidermal growth factor 2 positivity was significantly associated with malignant mass-associated NME. Although our study did not confirm this association, our results revealed significant associations between malignant mass-associated NME outcomes and lower Ki-67 indexes, which was an unexpected finding. Ki-67 index serves as a marker of cellular proliferation and is an independent prognostic metric for breast cancer survival outcomes (20). The relationship

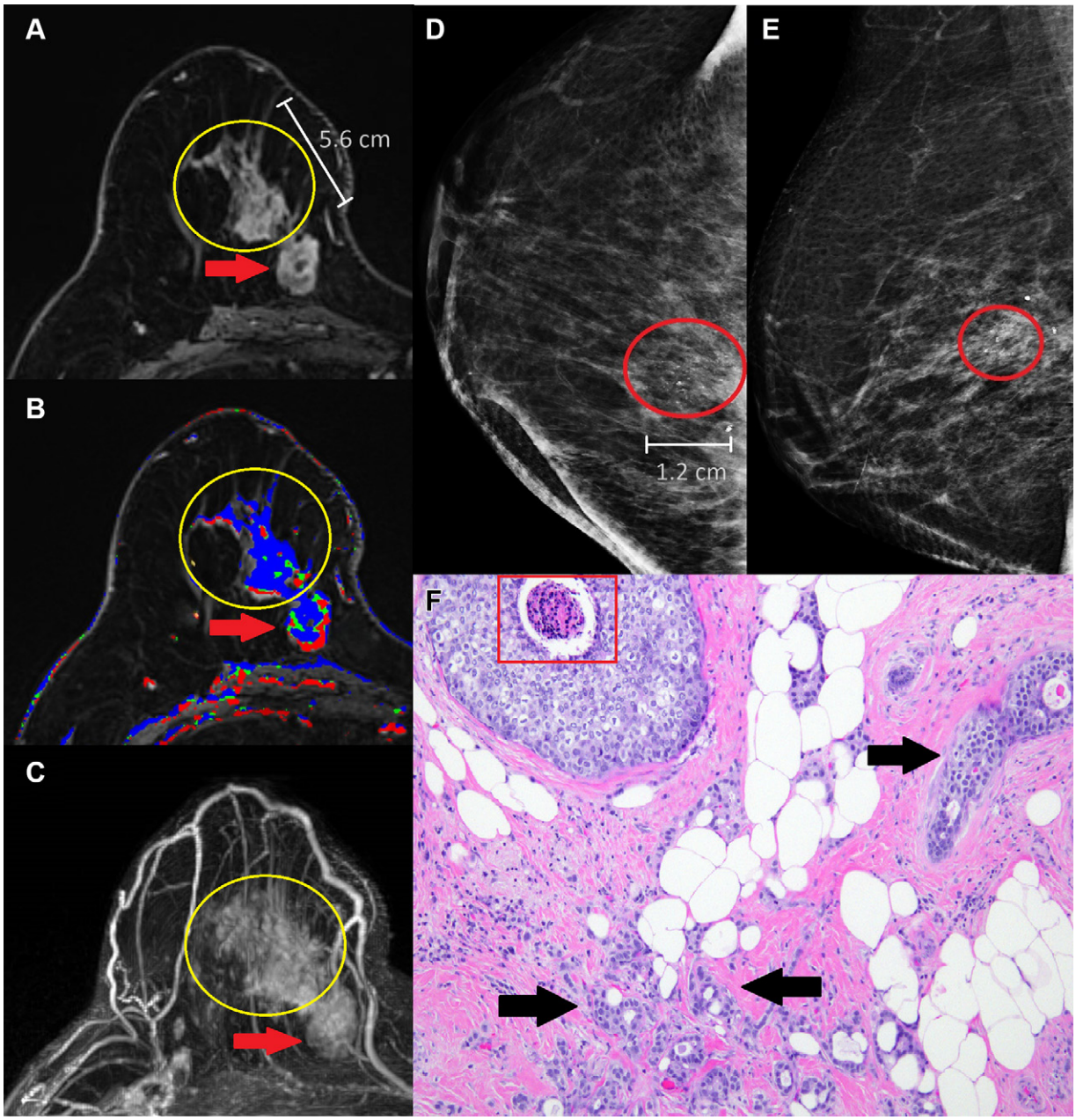

Figure 3: Mass-associated nonmass enhancement (NME) that was mastectomy-proven invasive ductal carcinoma (IDC) and ductal carcinoma in situ (DCIS) in a 58-year-old woman with newly diagnosed IDC. **(A)** Axial postcontrast T1-weighted subtraction image demonstrates a 5.6-cm heterogeneous NME in a segmental distribution (yellow circle) with predominantly persistent kinetics **(B)** extending from a 2.7-cm irregular heterogeneous mass with irregular margins (red arrow) with predominantly washout kinetics in the lower inner right breast. **(C)** Maximum intensity projection image demonstrates the mass-associated NME (yellow circle) extending from the malignant index mass (red arrow) in the lower inner right breast. **(D)** Full craniocaudal and **(E)** mediolateral oblique views demonstrate 1.2-cm amorphous calcifications in a segmental distribution (red oval) that correlate with the mass-associated NME observed at breast MRI. **(F)** Histologic view of the mass-associated NME shows atypical epithelial cells with comedonecrosis (red box), compatible with DCIS, and infiltrative glandular proliferation with minimal cytologic atypia and desmoplastic stromal response (black arrows), compatible with IDC. (Hematoxylin-eosin stain; original magnification, ×100.)

between malignancies and Ki-67 is more understood at mammography. Spiculated masses identified at mammography are often low-grade malignancies with low Ki-67 indexes, whereas circumscribed masses are more frequently associated with high-grade malignancies and higher Ki-67 indexes (21–23). The current hypothesis for this difference is that the lower cellular proliferation observed in low-grade malignancies allows time for the malignant cells to invade the surrounding tissue, resulting in the pulling of adjacent normal Cooper ligaments into the tumor, which manifests as spiculations on mammograms (21). Conversely, higher cellular proliferation observed in high-grade malignancies prevents malignant cells from invading the surrounding tissue, leading to circumscribed margins. Extrapolating concepts from this hypothesis could explain our results for the association between low Ki-67 indexes and malignant mass-associated NME. With lower proliferation, the associated

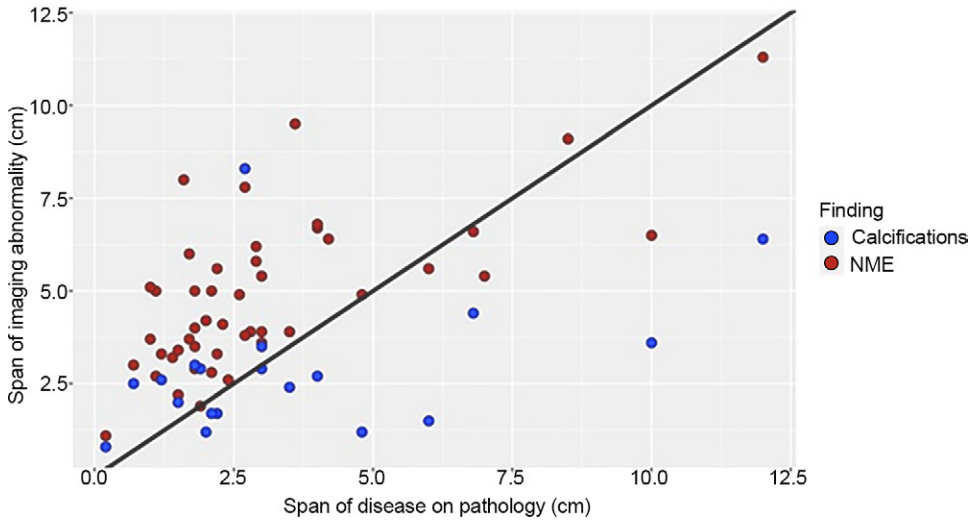

Figure 4: Scatterplot compares the span of suspicious imaging findings (y-axis) with the true histologic span (x-axis) in 41 patients with malignant index masses and mass-associated nonmass enhancement (NME) at preoperative MRI. Span of NME at MRI is indicated by red dots, and span of calcifications at mammography is indicated by blue dots. The black reference line demonstrates x = y.

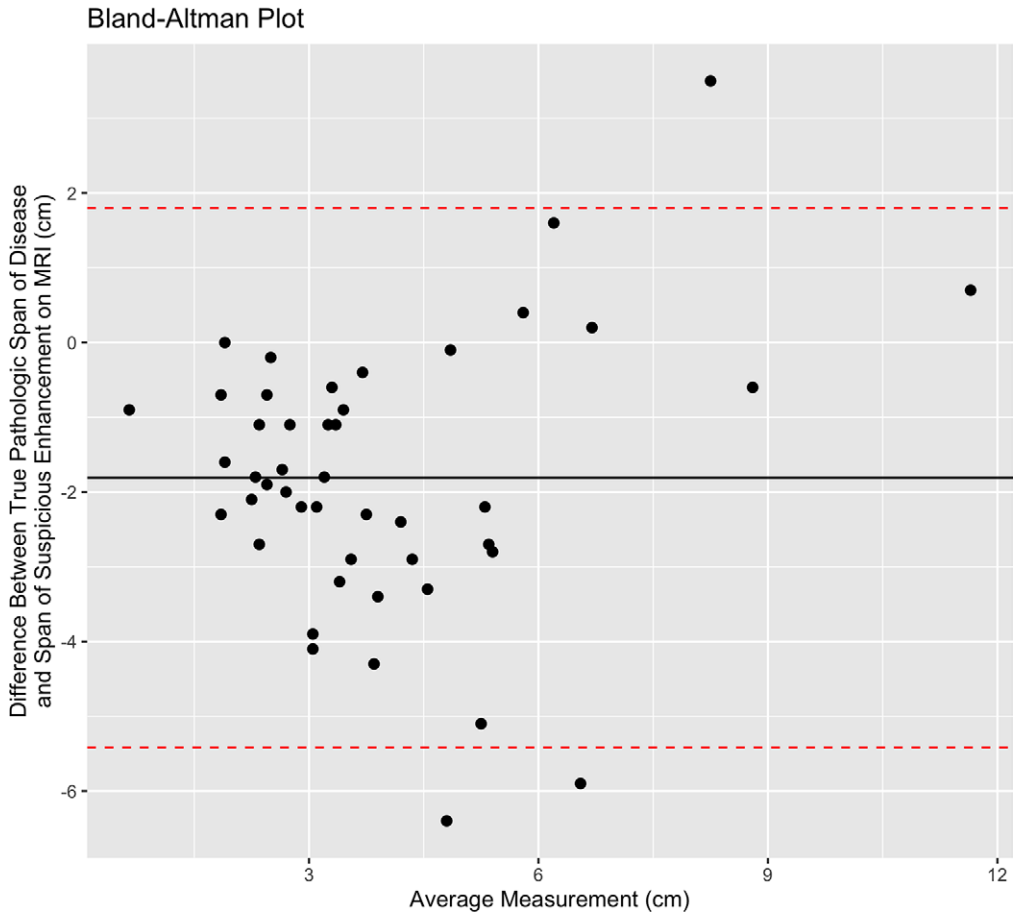

Figure 5: Bland-Altman plot shows the span of disease measured by pathologic analysis compared with the extent of suspicious imaging findings at MRI. The solid black line shows the mean difference between the two measurements, and the red dotted lines represent the 95% CIs.

malignant cells had time to invade the surrounding breast tissue and manifest as NME in a similar manner to the associated spiculations observed at mammography in low-grade malignancies. More studies on this are needed to understand the implications of mass-associated NME in the setting of low Ki-67 indexes versus high Ki-67 indexes.

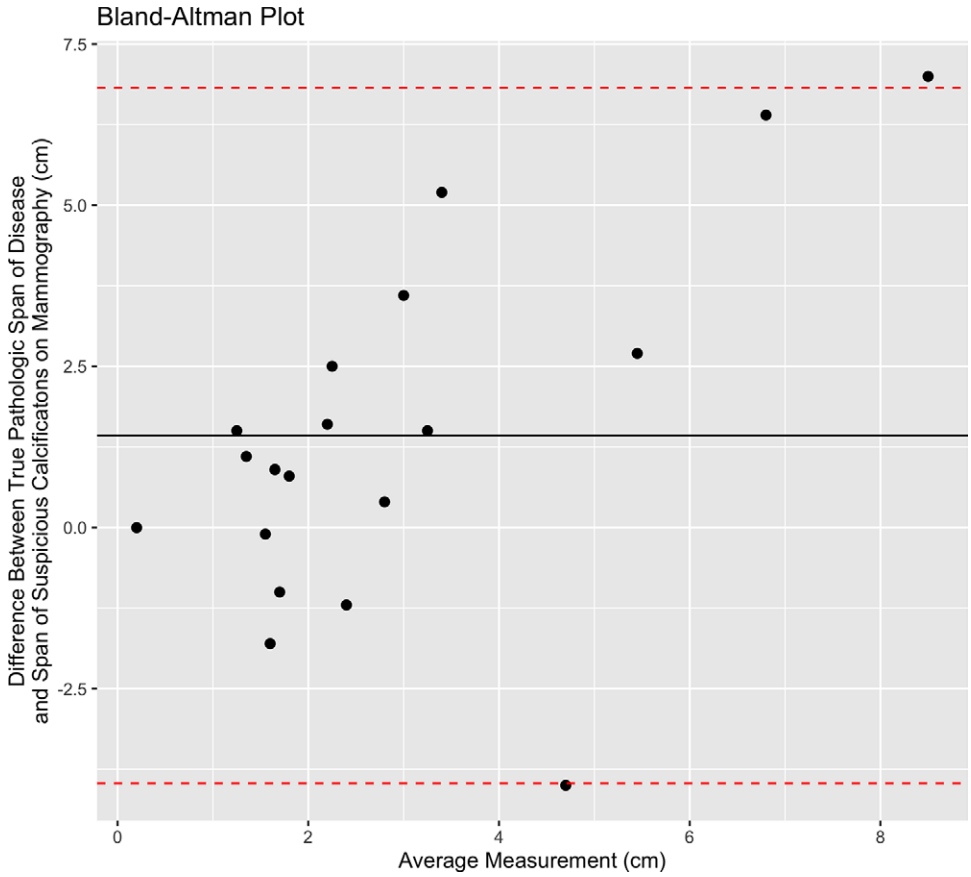

Figure 6: Bland-Altman plot shows the span of disease measured by pathologic analysis compared with the extent of suspicious imaging findings at mammography. The solid black line shows the mean difference between the two measurements, and the red dotted lines represent the 95% CIs.

We found that the span of disease measured at breast MRI overestimated the true extent of disease found at histologic evaluation. This is consistent with several previous studies demonstrating that MRI overestimates tumor size, especially in the setting of NME (24–26). Overestimation of disease at MRI has a substantial impact on patient care and surgical planning. Previous studies have reported that preoperative MRI findings prompted inappropriate conversions from breast-conserving surgery to wider excisions and mastectomies in up to 5%–8% of cases, with mastectomies (5%–11%) more frequent than wider excisions (2%–5%) (5–7). However, it is important to note that it is false-positive preoperative MRI findings that have resulted in a negative impact. True-positive MRI findings have resulted in 11% of appropriate conversions (5). MRI-guided biopsy recommendations of the distal margins of the mass-associated NME or two-site MRI-guided biopsy along the course of the mass-associated NME could be considered to prove the extent of disease. Breast radiologists need to work closely with breast surgeons to optimize the workup for these findings to optimize surgical planning.

Given the reported low specificity of NME at MRI, it would be helpful to determine imaging features associated with malignancy to increase positive predictive values in the preoperative setting (5,15). Gweon et al (19) previously determined that no imaging characteristic of mass-associated NME was significantly associated with a malignant pathologic condition. Our results support these findings, as no morphology, distribution, or kinetics of the mass-associated NME was significantly associated with a malignant pathologic condition. However, segmental distribution was the most common distribution reported for malignant mass-associated NME, but this did not meet statistical significance (P = .07). Traditionally, segmental distribution of NME is the most significant predictor of malignancy of all the NME distribution patterns (10,27). Larger cohort studies should be performed to further evaluate the association between mass-associated NME distribution and malignancy.

Surprisingly, both benign and malignant mass-associated NME had type 1 kinetics in most cases. While type 1 kinetics was previously thought to be associated with benignity, more recent studies have demonstrated that DCIS typically demonstrates nonsuspicious kinetics, and invasive lobular carcinoma rarely demonstrates suspicious kinetics (28,29). This suggests that kinetic analysis may not be reliable in the assessment of mass-associated NME or of NME in general. More data on using kinetic evaluation of preoperative MRI NME findings are needed to better inform clinical decision-making.

A subset of patients in our study had calcifications that correlated with the NME, and the majority of these were malignant. However, there was not a significant association

between mass-associated NME being malignant and the presence of correlating calcifications. Our results suggest that calcifications, if present, can be used as a target for stereotactic biopsy, obviating MRI-guided biopsy. In addition, calcification span at preoperative mammography may have an increased role in surgical planning when coupled with NME findings at preoperative MRI, as the span of calcifications (when present) was similar to the histologic span of disease. Future studies investigating the relationship between calcifications and NME in the preoperative setting are warranted.

Our study had important limitations. This study was performed at a single multisite academic institution. The small cohort size limits the value of overall and subset analyses. Larger studies are warranted to confirm our findings. Excluding the 12 cases without pathologist review may have affected our analysis of the span of disease. Our exclusion of patients who underwent neoadjuvant chemotherapy, which represents a unique subset of patients with breast cancer, may have also affected our results. As the pathologist was not blinded to the size of the mass-associated NME, this could have potentially introduced bias. The size discrepancy between the specimen at MRI and the pathologic specimen could be in part related to sequential shrinkage in specimen size from fresh specimen to formalin fixation and staining (30,31).

In conclusion, we found that NME contiguous with malignant index masses is clinically significant, yielding a malignant pathologic finding in more than half of cases. However, the total span of suspicious enhancement measured at MRI overestimated the true histologic span of disease. We recommend a multidisciplinary approach to evaluating these cases. Breast radiologists should work closely with breast surgeons to determine which patients would benefit from MRI-guided biopsy to guide appropriate surgical planning. We are optimistic that this study may provide evidence to avoid inappropriate conversions to wider excisions or mastectomy, as well as to limit positive margins. This could result in improved quality of personalized care among patients newly diagnosed with breast cancer with accompanying NME at preoperative MRI examinations.

Author contributions: Guarantors of integrity of entire study, **D.L.N., M.L., E.B.A.**; study concepts/study design or data acquisition or data analysis/interpretation, all authors; manuscript drafting or manuscript revision for important intellectual content, all authors; approval of final version of submitted manuscript, all authors; agrees to ensure any questions related to the work are appropriately resolved, all authors; literature research, **D.L.N., M.L., A.C.M., E.B.A.**; clinical studies, **D.L.N., M.L., A.C.M., E.B.A.**; statistical analysis, **E.B.A.**; and manuscript editing, all authors

Disclosures of conflicts of interest: **D.L.N.** American Roentgen Ray Society (ARRS) Resident in Radiology Melissa Rosado de Christenson Award at 2022 ARRS Annual Meeting ($2000 honoraria), Wendell Scott Research Award for Outstanding Research by a Breast Imaging Fellow at the 2023 Society of Breast Imaging/American College of Radiology Annual Meeting ($1000 honoraria); consultant for Hologic. **M.L.** No relevant relationships. **A.C.M.** Research grant to author's institution from Bristol-Myers Squibb. **M.H.** No relevant relationships. **E.B.A.** No relevant relationships.

References

1. How common is breast cancer? American Cancer Society. https://www.cancer.org/cancer/breast-cancer/about/how-common-is-breast-cancer.html. Accessed November 15, 2021.
2. Zhu X, Cao Y, Li R, Zhu M, Chen X. Diagnostic performance of mammography and magnetic resonance imaging for evaluating mammographically visible breast masses. J Int Med Res 2021;49(9):300060520973092.
3. Orel SG, Schnall MD. MR imaging of the breast for the detection, diagnosis, and staging of breast cancer. Radiology 2001;220(1):13–30.
4. Fischer U, Zachariae O, Baum F, von Heyden D, Funke M, Liersch T. The influence of preoperative MRI of the breasts on recurrence rate in patients with breast cancer. Eur Radiol 2004;14(10):1725–1731.
5. Plana MN, Carreira C, Muriel A, et al. Magnetic resonance imaging in the preoperative assessment of patients with primary breast cancer: systematic review of diagnostic accuracy and meta-analysis. Eur Radiol 2012;22(1):26–38.
6. Houssami N, Ciatto S, Macaskill P, et al. Accuracy and surgical impact of magnetic resonance imaging in breast cancer staging: systematic review and meta-analysis in detection of multifocal and multicentric cancer. J Clin Oncol 2008;26(19):3248–3258.
7. Sardanelli F, Trimboli RM, Houssami N, et al. Magnetic resonance imaging before breast cancer surgery: results of an observational multicenter international prospective analysis (MIPA). Eur Radiol 2022;32(3):1611–1623.
8. Liberman L, Morris EA, Dershaw DD, Abramson AF, Tan LK. MR imaging of the ipsilateral breast in women with percutaneously proven breast cancer. AJR Am J Roentgenol 2003;180(4):901–910.
9. Liberman L, Morris EA, Kim CM, et al. MR imaging findings in the contralateral breast of women with recently diagnosed breast cancer. AJR Am J Roentgenol 2003;180(2):333–341.
10. Rosen EL, Smith-Foley SA, DeMartini WB, Eby PR, Peacock S, Lehman CD. BI-RADS MRI enhancement characteristics of ductal carcinoma in situ. Breast J 2007;13(6):545–550.
11. Greenwood HI, Heller SL, Kim S, Sigmund EE, Shaylor SD, Moy L. Ductal carcinoma in situ of the breasts: review of MR imaging features. RadioGraphics 2013;33(6):1569–1588.
12. Di Ninno AAM, Mello GGN, Torres US, et al. MRI as a complementary tool for the assessment of suspicious mammographic calcifications: Does it have a role? Clin Imaging 2021;74:76–83.
13. Kang JH, Youk JH, Kim JA, et al. Identification of preoperative magnetic resonance Imaging features associated with positive resection margins in breast cancer: a retrospective study. Korean J Radiol 2018;19(5):897–904.
14. Bahl M, Baker JA, Kinsey EN, Ghate SV. MRI predictors of tumor-positive margins after breast-conserving surgery. Clin Imaging 2019;57:45–49.
15. Baltzer PA, Benndorf M, Dietzel M, Gajda M, Runnebaum IB, Kaiser WA. False-positive findings at contrast-enhanced breast MRI: a BI-RADS descriptor study. AJR Am J Roentgenol 2010;194(6):1658–1663.
16. Types of Breast Cancer. Breastcancer.org. https://www.breastcancer.org/types. Accessed December 26, 2021.
17. Harbeck N, Rastogi P, Martin M, et al. Adjuvant abemaciclib combined with endocrine therapy for high-risk early breast cancer: updated efficacy and Ki-67 analysis from the monarchE study. Ann Oncol 2021;32(12):1571–1581.
18. Morris EA, Comstock CE, Lee CH, et al. ACR BI-RADS Magnetic Resonance Imaging. In: ACR BI-RADS Atlas, Breast Imaging Reporting and Data System. Reston, Va: American College of Radiology, 2013.
19. Gweon HM, Jeong J, Son EJ, Youk JH, Kim JA, Ko KH. The clinical significance of accompanying NME on preoperative MR imaging in breast cancer patients. PLoS One 2017;12(5):e0178445.
20. Inwald EC, Klinkhammer-Schalke M, Hofstädter F, et al. Ki-67 is a prognostic parameter in breast cancer patients: results of a large population-based cohort of a cancer registry. Breast Cancer Res Treat 2013;139(2):539–552.
21. Liu S, Wu XD, Xu WJ, Lin Q, Liu XJ, Li Y. Is there a correlation between the presence of a spiculated mass on mammogram and luminal a subtype breast cancer? Korean J Radiol 2016;17(6):846–852.
22. Gao B, Zhang H, Zhang SD, et al. Mammographic and clinicopathological features of triple-negative breast cancer. Br J Radiol 2014;87(1039):20130496.
23. Zhu X, Chen L, Huang B, et al. The prognostic and predictive potential of Ki-67 in triple-negative breast cancer. Sci Rep 2020;10(1):225.
24. Grimsby GM, Gray R, Dueck A, et al. Is there concordance of invasive breast cancer pathologic tumor size with magnetic resonance imaging? Am J Surg 2009;198(4):500–504.
25. Onesti JK, Mangus BE, Helmer SD, Osland JS. Breast cancer tumor size: correlation between magnetic resonance imaging and pathology measurements. Am J Surg 2008;196(6):844–848; discussion 849–850.
26. Rominger M, Berg D, Frauenfelder T, Ramaswamy A, Timmesfeld N. Which factors influence MRI-pathology concordance of tumour size measurements in breast cancer? Eur Radiol 2016;26(5):1457–1465.

27. Lunkiewicz M, Forte S, Freiwald B, Singer G, Leo C, Kubik-Huch RA. Interobserver variability and likelihood of malignancy for fifth edition BI-RADS MRI descriptors in non-mass breast lesions. Eur Radiol 2020;30(1):77–86.
28. Kim JA, Son EJ, Youk JH, et al. MRI findings of pure ductal carcinoma in situ: kinetic characteristics compared according to lesion type and histopathologic factors. AJR Am J Roentgenol 2011;196(6):1450–1456.
29. Mann RM, Hoogeveen YL, Blickman JG, Boetes C. MRI compared to conventional diagnostic work-up in the detection and evaluation of invasive lobular carcinoma of the breast: a review of existing literature. Breast Cancer Res Treat 2008;107(1):1–14.
30. Tran T, Sundaram CP, Bahler CD, et al. Correcting the shrinkage effects of formalin fixation and tissue processing for renal tumors: toward standardization of pathological reporting of tumor size. J Cancer 2015;6(8):759–766.
31. Yeap BH, Muniandy S, Lee SK, Sabaratnam S, Singh M. Specimen shrinkage and its influence on margin assessment in breast cancer. Asian J Surg 2007;30(3):183–187.